Supporting Information

Design of lanthanide-based OLEDs with remarkable circularly polarized electroluminescence

Francesco Zinna[a], *Mariacecilia Pasini*[b], *Francesco Galeotti*[b], *Chiara Botta*[b], *Lorenzo Di Bari*[a,*] *and Umberto Giovanella*[b,*]

Table S1. Photophysical parameters of chiral Eu-complexes in solution.

emitter	PL-QY (%)	τ_{obs} (μs)	PL-QY$_{intr}$	η_{sens} [S1] (%)
CsEu(*(-)*-hfbc)$_4$	3.5	150	0.09	16.3

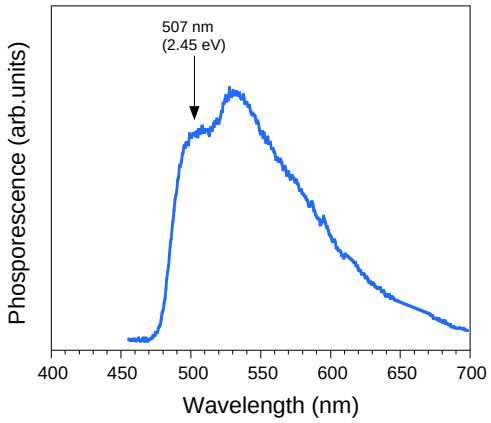

Figure S1. Phosphorescence of CsGd(*(–)*-hfbc)$_4$ frozen solution. According to the common procedure,[S2] the triplet level of CsEu((−)-hfbc)$_4$ was determined by measuring the phosphorescence of the isostructural complex[S3] CsGd((−)-hfbc)$_4$. In fact, unlike Eu(III), Gd(III) ion has no electronic level able to accept energy from the ligand triplet level and so no Ln-centred emission can be observed but just the phosphorescence of the ligand. The spectrum was measured in a CH_2Cl_2 (degassed) frozen solution at 77 K by a modified NanoLog-TCSPC by Horiba Italia S.r.l.

Table S2. HOMO, LUMO, energy levels and charge carrier mobility of host materials.

Compounds	HOMO (eV)	LUMO (eV)	triplet energy $T_1 \rightarrow S_0$ (eV)	Charge carrier Mobility (cm^2/Vs) h	e	REF.
TCTA	-5.7	-2.3	2.8	$\sim 10^{-4}$	/	[S4, S5]
OXD7	-6.2	-2.6	/	/	$\sim 10^{-5}$	[S6]

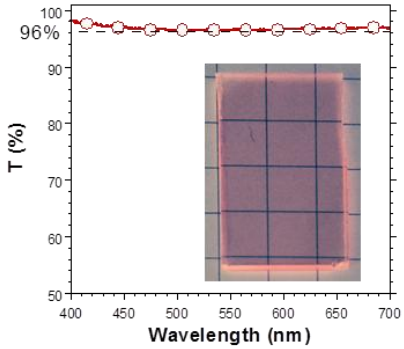

Figure S2. Transmittance of TCTA:OXD7:12wt.% CsEu(*(–)*-hfbc)$_4$ film on glass; inset, image of the film under UV light measured by Perkin-Elmer Lambda 900 UV-Vis-NIR spectrophotometer.

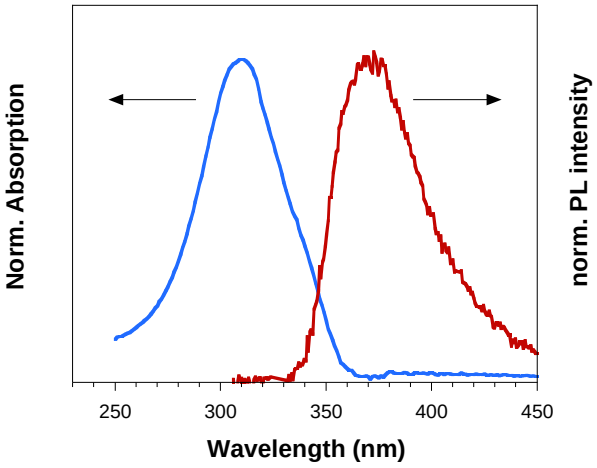

Figure S3. Absorption spectra of CsEu(*(–)*-hfbc)$_4$ solution (blu line) and PL spectra of TCTA:OXD7 film (red line).

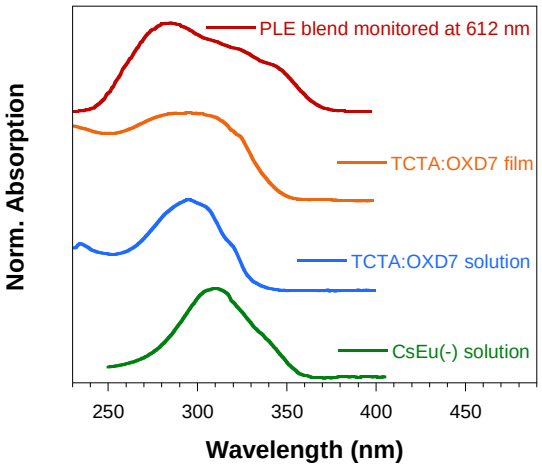

Figure S4. Absorption spectra of TCTA:OXD7 (solution and film) and CsEu((–)-hfbc)$_4$ (solution) and PLE spectrum of TCTA:OXD7:CsEu((–)-hfbc)$_4$ film monitored at 612 nm.

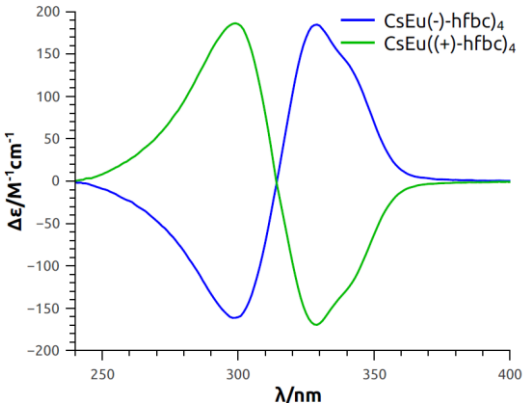

Figure S5. ECD for CsEu(hfbc)$_4$ in $CHCl_3$ solution.

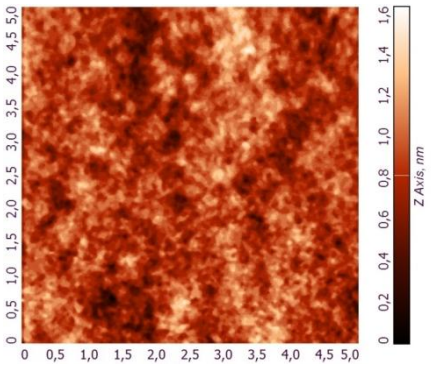

Figure S6. AFM tapping mode 5 m x 5 m image of TCTA:OXD7:CsEu((–)-hfbc)$_4$ film.

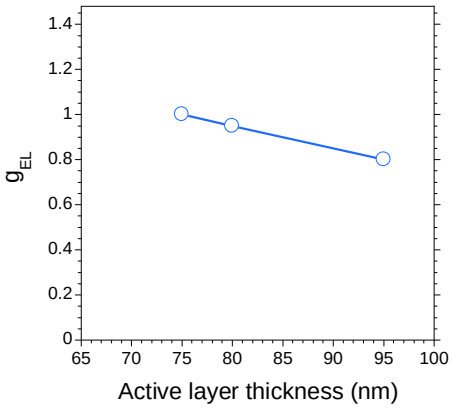

Figure S7. g_{EL} behavior *vs* active layer thickness. Single layer CP-OLEDs with different active layer thickness were fabricated. Due to the pretty high operational voltage of semitransparent devices without CIL (> 15-18 V) , the thickness of the active layer cannot be increased above ~100 nm to maintain good reproducibility of the performance. The thickness had no effect on g_{PL} of uncovered films (-1.21±0.02 at 595 nm for both 75 and 100 nm films) while a reduction of g_{EL} was observed as the thickness increased. Besides the highest g_{EL} = 1 for ~75 nm thick device A, values of -0.95 and 0.11 at 595 and 612 nm respectively for ~ 80 nm thick device, and -0.8 and 0.04 at 595 and 612 nm respectively for ~ 95 nm thick active layer device were measured.

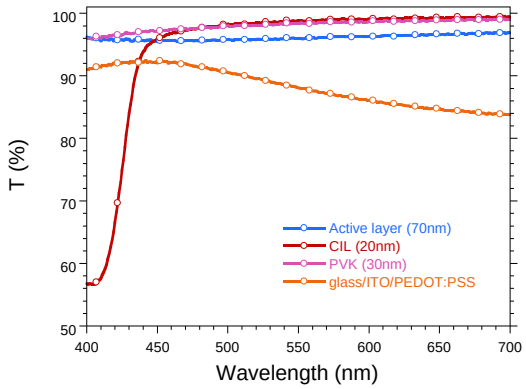

Figure S8. Transmittance spectra of the various layers of the device

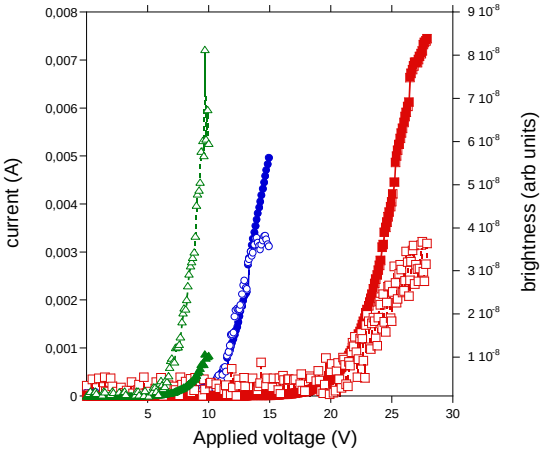

Figure S9. Representative current (filled symbols)-brightness (empty symbols)-voltage characteristics of ITO/PEDOT/ TCTA:OXD7:12wt.% CsEu(*(–)*-hfbc)$_4$ /Ba/Al (blue), ITO/PEDOT/AIL/ TCTA:OXD7:12wt.% CsEu(*(–)*-hfbc)$_4$ /Ba/Al (red) and ITO/PEDOT/ TCTA:OXD7:12wt.% CsEu(*(–)*-hfbc)$_4$/CIL/Ba/Al (green) devices with semitransparent cathode.

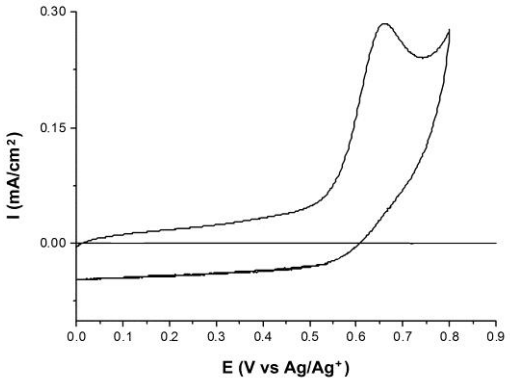

Figure S10. Cyclic voltammogram of the complex CsEu((–)-hfbc)4 recorded vs Ag/Ag+ in acetonitrile at 298 K (scan rate: 100 mV·s^{-1}), TBAP, CG 0.06 cm2. The HOMO level was calculated using the equation: E (HOMO) = 4.39 + E_{ox} (SCE). The LUMO level was derived by optical gap.

Effects of the electrodes-recombination zone (RZ) position on the polarization efficiency.
As in our previous model,[S7] we consider that half of the radiation is emitted forward and half backward. According to Beer–Lambert law, the emitted light (I_0) is attenuated exponentially with the distance x between the anode (where the light exits the device) and the recombination zone, where the photon is generated:

$$I = I_0 e^{-\alpha x} \qquad \text{(eq. S1)}$$

where α is the attenuation coefficient of the all the layers between the anode and the cathode. Eq. (S1) is related to the total transmittance T (including absorption, scattering and any other dissipation process) of the layers as $T = e^{-\alpha d}$.

In first approximation, we shall consider that the light is emitted only by an infinitesimally thin layer of the active layer (see Figure S11). The loss of the fraction of the light emitted backward and forward varies with the distance of the recombination zone from the cathode according to eq. (S1). The backward component eventually undergoes reflection on the cathode, and therefore its handedness is reversed.

The pathway traveled by the backward light is conveniently divided into three steps:

- In the way between the RZ and the cathode, it is attenuated by a factor $e^{-\alpha(d-x)}$.
- Owing to the reflection on the cathode surface it is further attenuated by a factor R (reflectance) and its handedness is reversed.
- In the way back from the cathode to the anode, it is finally attenuated by a factor $e^{-\alpha d}$.

The total attenuation factor is therefore:

$$R \cdot e^{-\alpha(2d-x)} \qquad \text{(eq. S2)}$$

Applying these attenuation factors to the two intrinsic polarized component ($I_L^{(0)}$ and $I_R^{(0)}$) and taking into account the sign reversal of the polarization after reflection, we have that the two polarized components exiting the device (I_L' and I_R') are:

$$I_L' = \frac{1}{2} I_L^{(0)} \cdot e^{-\alpha x} + \frac{1}{2} I_R^{(0)} \cdot R \cdot e^{-\alpha(2d-x)} \qquad \text{(eq. S2a)}$$

$$I_R' = \frac{1}{2} I_R^{(0)} \cdot e^{-\alpha x} + \frac{1}{2} I_L^{(0)} \cdot R \cdot e^{-\alpha(2d-x)} \qquad \text{(eq. S2b)}$$

Where $I_L^{(0)}$ and $I_R^{(0)}$ are the intrinsic polarization components emitted by the chiral molecule. Factor ½ is needed because half of the light is emitted forward and half backward.

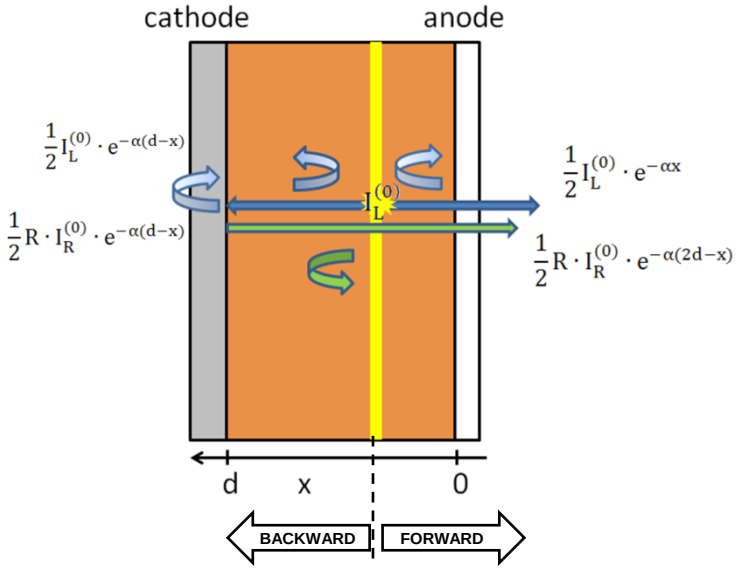

Figure S11: Schematic representation of a device. The yellow strip represents the recombination zone, curved arrows represent light losses. Light before reflection is indicated in blue, light after reflection is indicated in green. On top of each arrow, we report the attenuation for the left polarized component.

The overall g_{EL} factor that we measure for the device is:

$$g_{EL} = 2\frac{I'_L - I'_R}{I'_L + I'_R} \qquad \text{(eq. S3)}$$

By substituting eq. (S2a) and (S2b) in eq. (S3) and rearranging the terms, we obtain:

$$g_{EL} = 2\frac{e^{-\alpha x}\left(I_L^{(0)} - I_R^{(0)}\right) - R\cdot e^{-\alpha(2d-x)}\left(I_L^{(0)} - I_R^{(0)}\right)}{e^{-\alpha x}\left(I_L^{(0)} + I_R^{(0)}\right) + R\cdot e^{-\alpha(2d-x)}\left(I_L^{(0)} + I_R^{(0)}\right)} = 2\frac{\left(I_L^{(0)} - I_R^{(0)}\right)}{\left(I_L^{(0)} + I_R^{(0)}\right)} \cdot \frac{e^{-\alpha x} - R\cdot e^{-\alpha(2d-x)}}{e^{-\alpha x} + R\cdot e^{-\alpha(2d-x)}} \text{ (eq. S4)}$$

We note that $2\frac{\left(I_L^{(0)} - I_R^{(0)}\right)}{\left(I_L^{(0)} + I_R^{(0)}\right)} = g_{EL}^{(0)}$, i.e. the intrinsic g factor of the chiral emitter, and by substituting it in eq. (S4), after multiplying both the numerator and denominator by $e^{+\alpha x}$, we get:

$$g_{EL} = g_{EL}^{(0)}\frac{1 - R\cdot e^{-2\alpha(d-x)}}{1 + R\cdot e^{-2\alpha(d-x)}} \qquad \text{(eq. 1)}$$

Eq. (1) shows that g_{EL} monotonously increases with x, meaning that higher g_{EL}-s are expected when the recombination zone is close to the anode interface.
It is worth noting that when the recombination occurs very close to the anode (x = 0), eq. (1) becomes:

$$g_{EL} = g_{EL}^{(0)}\frac{1 - R\cdot e^{-2\alpha d}}{1 + R\cdot e^{-2\alpha d}} \qquad \text{(eq. S5)}$$

Since $e^{-\alpha d} = T$, i.e. the overall transmittance of the active layer and the CIL, eq. (S5) becomes:

$$g_{EL} = g_{EL}^{(0)} \frac{1-R \cdot T^2}{1+R \cdot T^2} \qquad \text{(eq. S6)}$$

In the opposite case, when the recombination occurs very close to the cathode (x = d), we have:

$$g_{EL} = g_{EL}^{(0)} \frac{1-R}{1+R} \qquad \text{(eq. S7)}$$

Equation S7 is the equation worked out in our previous model, which did not take into account loss of radiation within the layers between anode and cathode.

Plotting eq. (1) with reasonable values for semitransparent device ($g_{EL}^{(0)} = 1.38$, $T = 0.9$, $R = 0.38$, for a 6 nm Al cathode[S8]), the g_{EL} can vary as much as 15-20% as an effect only of the recombination zone position (roughly from ≈ 0.6 to ≈ 0.7). For the sake of comparison, in Table S3 we show the experimental g_{EL} values obtained for different architecture sorted by RZ position.

Table S3. Experimental g_{EL} values obtained for different architecture sorted by RZ position and expected g_{EL} in the two limit cases as predicted by eq. (S6) and eq. (S7).

RZ near to the	device[a]	Experimental g_{EL}	Calculated g_{EL}
cathode	AIL/TCTA:OXD7	0.61	0.63
	AIL/TCTA	0.6	
anode	TCTA:OXD7/CIL	0.88	0.74
	TCTA:OXD7	1/0.8[b]	

[a] semitransparent cathode; [b] 100 nm active layer thickness

However, when the recombination zone can not be approximated to be reasonably thin with respect to the active layer thickness[S9], eq. (1) should be integrated over the whole active layer, after being weighted with a function $\rho = \rho(x)$ describing the spatial distribution of the recombination zone:

$$g_{EL} = \int_0^d g_{EL}^{(0)} \frac{1-R \cdot e^{-2\alpha(d-x)}}{1+R \cdot e^{-2\alpha(d-x)}} \rho(x)\, dx \qquad \text{(eq. S8)}$$

[S1] C. Freund, W. Porzio, U. Giovanella, F. Vignali, M. Pasini, S. Destri, A. Mech, S. Di Pietro, L. Di Bari, and P. Mineo, *Inorganic Chemistry*, 2011. **50**, 5417.

[S2] K. Binnemans, Coord. Chem. Rev., 2015, **295**, 1.

[S3] S. Di Pietro, L. Di Bari, *Inorg. Chem.*, 2012, **51**, 12007.

[S4] S. Höfle, C. Bernhard, M. Bruns, C. Kübel, T. Scherer, U. Lemmer, and A. Colsmann, *ACS Appl. Mater. Interfaces* 2015, **7**, 20769.

[S5] D. P.-K. Tsang, M.-Y. Chan, A. Y.-Y. Tam, V. W.-W. Yam, *Org. Electron*. 2011, **12**, 1114.

[S6] Y.-T. Chang, J.-K. Chang, Y.-T. Lee, P.-S. Wang, J.-L. Wu, C.-C. Hsu, I-W. Wu, W.-H. Tseng, T.-W. Pi, C.-T.Chen, and C.-I Wu, *ACS Appl. Mater. Interfaces* 2013, **5**, 10614.

[S7] F. Zinna, U. Giovanella, L. Di Bari, *Adv Mater* **2015**, *27*, 1791.

[S8] F G. Hass, J. E. Waylonis, *J. Opt. Soc. Am*.1961, **51**, 719.

[S9] N. C. Erickson, and R. J. Holmes, *Adv. Funct. Mater.* 2013, **23**, 5190.